A review on the electrochemical reduction of CO_2 in fuel cells, metal electrodes and molecular catalysts

Rern Jern Lim[1], Mingshi Xie[1], Mahasin Alam Sk[1],

Jong-Min Lee[1], Adrian Fisher[2], Xin Wang[1], Kok Hwa Lim[1,*]

[1]*Division of Chemical and Biomolecular Engineering, School of Chemical and Biomedical Engineering, Nanyang Technological University, Singapore 637459, Singapore*

[2]*Department of Chemical Engineering and Biotechnology, University of Cambridge, New Museums Site, Pembroke Street, Cambridge, CB2 3RA, UK*

ABSTRACT

In this review article, we report the development and utilisation of fuel cells, metal electrodes in aqueous electrolyte and molecular catalysts in the electrochemical reduction of CO_2. Fuel cells are able to function in both electrolyser and fuel cell mode and could potentially reduce CO_2 and produce energy at the same time. However, it requires considerably high temperatures for efficient operation. Direct reduction using metal electrodes and molecular catalysts are possible at room temperatures but require an additional applied potential and generally have low current densities. Density functional theory (DFT) studies have been used and have begun to unveil possible mechanisms involved which could lead to improvements and development of more efficient catalysts.

Keywords: CO_2 reduction, Electrochemistry, Fuel cells, Metal electrodes, Molecular catalysts.

Corresponding Author: Email: kokhwa@ntu.edu.sg, Tel:+65-65141909, Fax:+65-67947553

1. Introduction

Since the industrial revolution, atmospheric carbon dioxide (CO_2) level of about 278 ppm has continuously increased due to extensive use of fossil fuels [1]. Recent report showed that atmospheric CO_2 level has reached the 400 ppm mark [2] and it is expected to continue to rise. The climate modelling study performed by Solomon et al. has shown that the effects of climate change due to the increase in greenhouse gases would have lasting effects of up to 1000 years even when there is zero emission of greenhouse gases [3-5]. Currently, the release of CO_2 into the environment is uncontrolled from various industrial and anthropogenic processes. The open loop nature of these processes which releases CO_2 into the environment is not only unsustainable; but is also contrary to the natural carbon cycle which is a closed loop process. Although the study by Solomon et al. [3, 4] do not take into account forced or artificial sequestration of greenhouse gases especially CO_2, it is still important that the release of CO_2 into the environment has to cease as soon as possible to minimize the adverse impact of climate change. Instead of sequestrating atmospheric CO_2 only, the captured CO_2 should also be turned into fuels which not only closes the open loop processes that we have but also reduces our dependency on fossil fuels. Various other potential uses for CO_2 in the industry has also been highlighted where the utilization of CO_2 may reach an upper limit of 700 Mt/yr [6]. Being able to efficiently turn CO_2 into fuels would have the largest benefit and impact in the effort to reduce CO_2 emissions. This is because 80% of our energy is derived from fossil fuels [7].

Energy from carbon neutral sources such as renewables and/or nuclear can be used to synthesize these fuels by storing the energy in a chemical form. Besides, it would be possible to utilize existing infrastructures to transport and store the fuels [8, 9]. Energy from renewables and nuclear is generally in the form of electricity, hence electrochemistry potentially plays an important role in the production of fuels from CO_2. The Fischer-Tropsch

(FT) process is also an important process in the endeavour to turn CO_2 into fuels. The FT process utilizes carbon monoxide (CO) and hydrogen (H_2) or synthesis gas (syngas) and produces hydrocarbons in the presence of iron or cobalt catalyst (Eq. 1) [10]. A side and competing reaction is the water-gas shift (WGS) reaction where CO_2 is produced instead (Eq. 2).

$$\mathrm{CO} + 2.15\mathrm{H_2} \rightarrow \text{hydrocarbons} + \mathrm{H_2O} \quad (1)$$

$$\mathrm{CO} + \mathrm{H_2O} \rightleftharpoons \mathrm{CO_2} + \mathrm{H_2} \quad (2)$$

Various studies in the electrochemical reduction of CO_2 have reported the formation of CO [11-13]. Studies on high temperature electrochemical reduction of CO_2 produces only CO and H_2 as main products, have good current densities and does not require an applied potential [12, 13]. The selectivity and production of CO in the aqueous electrochemical reduction of CO_2 at room temperature is dependent on the electrode material [11]. The main drawback of this process is that it requires an additional applied potential and relatively low current density. However, it is possible to obtain other products such as hydrocarbons, formate and alcohols from this process which is not possible in the high temperature electrochemical reduction process [14-18].

It is much more favourable thermodynamically to form stable molecules via proton-coupled multi-electron steps rather than single electron steps. However, the formation kinetics is not favourable as confirmed by other studies where higher applied potentials are required [14-18]. Briefly, equations 3-8 are used to estimate the standard reduction potential (with respect to the standard hydrogen electrode (SHE)) from formation energies in aqueous media at pH 7, atmospheric pressure and 25 °C [19].

$$\mathrm{CO_2} + \mathrm{e^-} \rightleftharpoons \mathrm{CO_2^-} \qquad (-1.90\mathrm{V}) \quad (3)$$

$$\mathrm{CO_2} + \mathrm{H_2O} + 2\mathrm{e^-} \rightleftharpoons \mathrm{CO} + 2\mathrm{OH^-} \qquad (-0.52\mathrm{V}) \quad (4)$$

$$\mathrm{CO_2} + 6\mathrm{H_2O} + 8\mathrm{e^-} \rightleftharpoons \mathrm{CH_4} + 8\mathrm{OH^-} \qquad (-0.25\mathrm{V}) \quad (5)$$

$$2CO_2 + 8H_2O + 12e^- \rightleftharpoons C_2H_4 + 12OH^- \qquad (-0.34V) \qquad (6)$$

$$2CO_2 + 9H_2O + 12e^- \rightleftharpoons C_2H_5OH + 12OH^- \qquad (-0.33V) \qquad (7)$$

$$3CO_2 + 13H_2O + 18e^- \rightleftharpoons C_3H_7OH + 18OH^- \qquad (-0.32V) \qquad (8)$$

Other than metal electrodes, metal complexes have also been studied for electrochemical reduction of CO_2. The three types of metal complexes for electrochemical reduction are metal complexes with (a) macrocyclic ligands, (b) bipyridine ligands and (c) phosphine complexes [20]. The combination of metal complexes with a gas diffusion electrode was found to have an extremely high current efficiency for the formation of CO [21].

In this article we review the works on the electrochemical reduction of CO_2 using solid oxide fuel cells, metal electrodes in aqueous solution and metal complexes and advances in understanding the mechanisms involved.

2. Solid Oxide Fuel Cells

Solid oxide fuel cells (SOFCs) have been studied extensively for the generation of power. The authors would like the readers to refer to the review by Choudhury et al. for the recent progress made in the study of SOFCs [22]. Briefly, SOFCs have the capability to generate power of up to 300 kW and up to several MW when combined with a steam or gas turbine. Efficiencies that could be achieved ranged from 50 – 80% depending on the design of the process. The types of fuels used are natural gas, methane or pure hydrogen with exhaust products consisting of mainly water, CO, CO_2, H_2 and heat. Methanol can also be used as fuel for SOFCs [23]. It is also possible to reduce CO_2 to CO by reforming with methane (Eq. 9) over rhodium, iridium or nickel [24]. This reforming process (dry reforming) is not only able to produce syngas with favourable H/CO ratios but may potentially reduce the amount of CO_2 in the environment [23].

$$CO_2 + CH_4 \rightarrow 2CO + 2H_2 \quad (9)$$

Reports of using CO_2 as a fuel in SOFCs have begun to increase in the recent years [12, 15, 25-32]. Nickel [13, 25, 27, 28], platinum [29-32], copper [12] and palladium [26] had been reported to be the active components. Despite having different active components, the main component of the electrolytes used is essentially the same which is non-porous yttria-stabilized zirconia (YSZ). The YSZ electrolyte functions as an oxygen ion conductor at very high temperatures (800-900 °C) [29]. This oxygen ion transfer phenomenon occurs due to the vacancies present in the crystal lattice of the electrolyte.

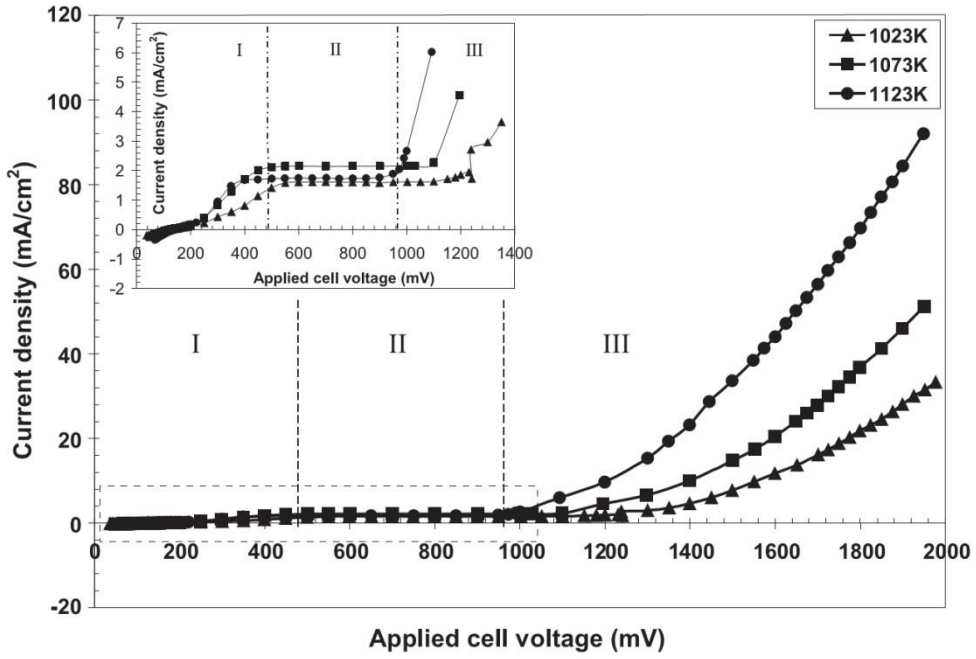

Fig. 1 CO_2 electrolysis current density vs. applied cell potential for Pt based SOFC. Roman numerals indicate low (I), constant (II) and high (III) current density regions. (Reproduced from ref. [31] by permission from Elsevier).

2.1. Platinum

Initially, the main goal of using SOFCs to reduce CO_2 was to produce oxygen from the CO_2 rich atmosphere of Mars in future missions; not energy [29, 30]. The electrolyte was

sandwiched between porous platinum electrodes and a potential of less than -2.0 V was applied to the cell. The current flow of this process was found to be completely due to the flow of oxygen ions and not due to electron transport [29]. Oxygen-containing species (OCS) present during electrolysis increased the resistance of the oxygen ion flow. Two main types of OCS that were identified are weakly adsorbed oxygen ($O^{\cdot\cdot}(Pt)_n$) and stable oxides ($O(Pt)_n$) [30]. The OCS partially blocks available sites for oxygen transfer at the electrode/electrolyte interface thus causing an increase in resistance of oxygen ion flow. Further studies were conducted to determine the rate determining steps and to improve the performance and efficiency of the cell [31, 32]. The rate determining step in the low and constant current density region was found to be the gas diffusion whereas in the high current density region it was the kinetics of CO_2 electrolysis (Fig. 1) [31]. Significant improvements were made using Pt-YSZ cermet electrodes which reduced the anode overpotentials, ohmic resistance and an increased electrochemical reaction at the interfaces [32].

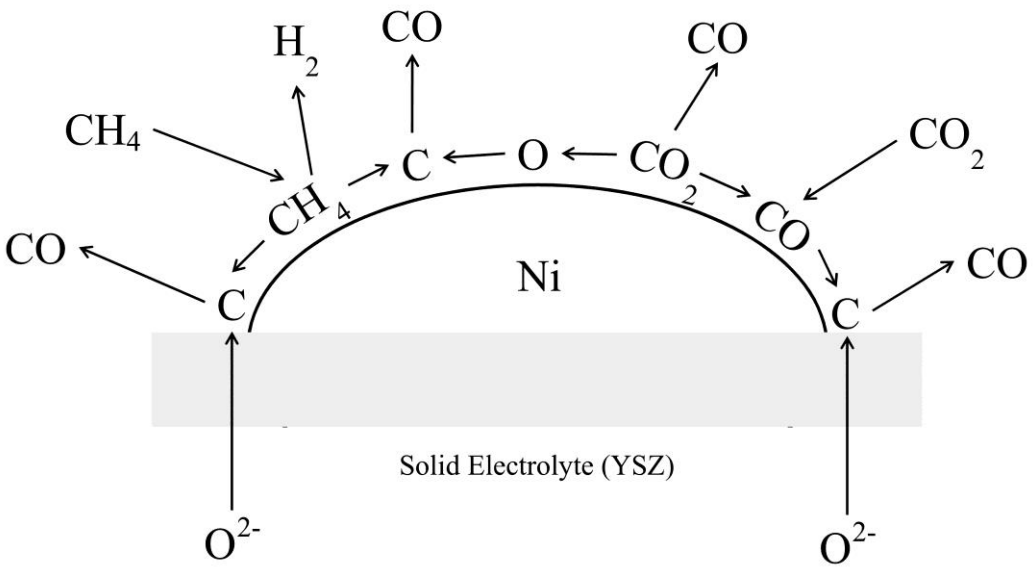

Fig. 2 Proposed mechanism for nickel based SOFC (Adapted from ref. [27] by permission from Elsevier).

2.2. Nickel

Due to the rarity and high prices of platinum which may affect commercialization, other researchers have turned their focus to use nickel as the active agent in the reduction of CO_2. Similar to platinum, initial study using nickel was to isolate oxygen therefore a potential is applied to perform the reduction process [25]. Methane formation was reported as the mixture of CO_2 and H_2 was used as fuel instead of pure CO_2 as in studies using platinum. Nickel supported on zeolite together with YSZ and silver electrodes was used. The zeolite present adsorbed CO_2 and facilitated the methanation process over the nickel particles through a one-step reaction (Eq. 10). It was postulated that (a) oxygen is first converted to water by the Ni/zeolite catalyst and then transferred through the YSZ electrolyte after the water is ionized, (b) CO_2 dissociation on the cathode electrode was not responsible for the formation of O_2 and (c) the rate determining step is the charge transfer process.

$$\mathrm{CO_{2,ad}} + 3\mathrm{H_2} \rightarrow \mathrm{CH_4} + \mathrm{H_2O} \tag{10}$$

The focus from oxygen production from CO_2 reduction then shifted to electrocatalytic dry reforming. This process does not require an applied potential and generates power. Kim et al. explored this concept and proposed a possible mechanism (see Fig. 2) [27]. Nickel cermet (Ni-YSZ-CeO) was used as the active electrode (anode) with feeds of CO_2/CH_4 mixture and pure H_2. The maximum power generated was 10.4 mW/cm^2 and 8.6 mW/cm^2 for pure H_2 and CO_2/CH_4 feeds, respectively. The occurrence of coking caused the performance of the cell to decrease during open circuit conditions via CH_4 decomposition and/or CO disproportion (Boudouard reaction) (Eq. 11, 12 respectively). However, during short circuit conditions, coking was suppressed due to the oxidation of surface carbon to CO and/or CO_2 by the oxygen ions.

$$\mathrm{CH_4} \rightleftharpoons 2\mathrm{H_2} + \mathrm{C_{ad}} \tag{11}$$

$$2\mathrm{CO} \rightleftharpoons \mathrm{CO_2} + \mathrm{C_{ad}} \tag{12}$$

Recently, Zhan et al. used a similar SOFC to Kim et al. and demonstrated that it is possible to use the cell reversibly as an electrolyser and a fuel cell [13]. The fuel source is a mixture of 25% H_2–75% CO_2 and managed to achieve a current density of 1.0 A/cm^2 at 1.30 V. It was postulated that steam undergoes reduction to H_2 (Eq. 13) and CO production proceeds through the reverse WGS reaction (Eq. 2) when in electrolyser mode.

$$H_2O + 2e^- \rightarrow O^{2-} + H_2 \quad (13)$$

Recent experimental and modelling studies at 650, 700 and 750 °C using CO/CO_2 mixtures revealed that carbon deposition is severe especially at the cathode/electrolyte interface when the cell is operated in electrolyser mode [33]. Dissociation of CO_2 and desorption of CO from the active Ni surface occur much easily at higher temperatures in both electrolyser and fuel cell mode.

2.3. Palladium

Although nickel is a much more economical choice for the use in SOFCs, it is prone to the formation of nickel carbonyls, coking and reoxidation of the electrode hence palladium was used to overcome these drawbacks [26]. A modified version of the electrode which is a mixed oxide of lanthanum-strontium-chromium-manganese (LSCM) with Pd/CZY (ceria-zirconia-yttria mixed oxide) was used and a power density of 0.45 W/cm^2 was achieved for a fuel mixture of equal parts of CO and CO_2.

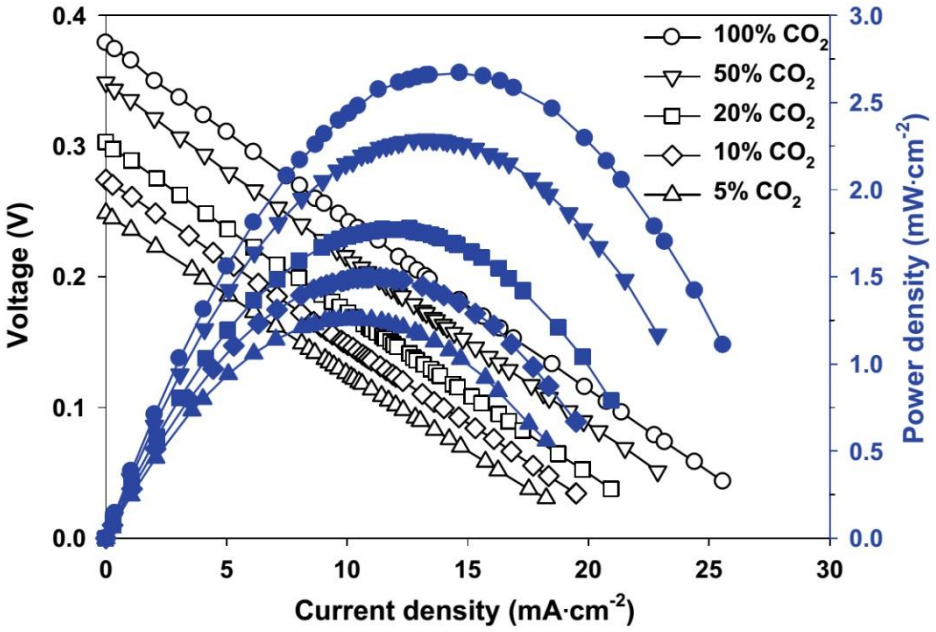

Fig. 3 Voltage-current and power-current profile for different CO_2 feed concentrations at a Cu based SOFC at 800 °C. (Reproduced from ref. [12] by permission from Elsevier).

2.4. Copper

Huang et al. proposed and demonstrated the use of copper in SOFCs as it was frequently used in the electrochemical reduction of CO_2 in aqueous solutions [12]. The mixed oxide of lanthanum-strontium-chromium-iron (LSCF) with gadolinia-doped ceria (GDC) impregnated with copper was used as the electrode. Pure CO_2 or CO_2/Argon mixture was used as the fuel which generated CO as product. Highest power density of 2.67 mW/cm^2 was achieved for pure CO_2 feed (see Fig. 3) and the production of CO increases with temperature and CO_2 feed concentration with no coking observed. It was postulated that in order to produce CO, the dissociation of CO_2 had to occur (Eq. 14). The reported activation energy for the reduction to occur was 2.72 kcal/mol which is much lower than values reported in heterogeneous catalysis [34].

$$CO_2 \rightarrow CO + O \qquad (14)$$

Recently, a similar study was performed with equal mixtures of CO and CO_2 as fuel in electrolyser mode at 750 °C [35]. It was found that CO oxidises at a higher rate compared to the reduction rate of CO_2. However, the current efficiency for CO production is 100% up to -1.5 V. At higher potentials (about > -2.3 V), there is an irreversible degradation to the solid electrolyte thus decreasing the efficiency of CO production.

2.5. Other

Xie et al. used a solid oxide electrolyser based with iron supported on iron oxide as a cathode, a solid electrolyte oxide mixture of barium, zinc, ceria, zirconia and yttria (BCZYZ) and Ni/BCZYZ as the anode [36]. This electrolyte behaves differently as compared to YSZ as it functions like a proton exchange membrane instead of oxygen ions. 3% H_2O/H_2 and pure CO_2 was fed to the anode and cathode, respectively. Major product from the process is CO while the minor product was methane. Current efficiencies for CO and methane were not very high at only 29.5% and 2.4%, respectively at very high applied potentials of -2.6 V and current density of 1.5 A/cm^2.

3. Metallic Electrodes in Aqueous Solution

Early studies into aqueous reduction on CO_2 using metallic electrodes began in the late 20^{th} century and have continued until today. In spite of the extensive literature, this method has yet to be commercialized, citing various drawbacks such as high overpotentials and production of mixed product [15]. Much of the focus had been on copper electrodes instead of other metals that have been tested. The reason behind this is the ability of copper to directly produce hydrocarbons and other products at a high current efficiency as compared to

other metals that tend to be very selective towards a single product; namely CO (Au, Ag, Zn, Ga, Pd), formate (Pb, Hg, In, Sn, Cd, Tl) or hydrogen only (Ni, Fe, pt, Ti) [11].

3.1. Copper

In 1985-1986, Hori et al. reported the ability of copper to produce hydrocarbons via electrochemical reduction of CO_2 [37, 38]. A current efficiency of 65% for methane formation was achieved at 0 °C but dropped rapidly with the rise in temperature while the current efficiency for ethylene steadily increased with temperature to about 20% at 40 °C. Doubling of the current density from 5 to 10 mA/cm^2 did not affect the current efficiencies for both methane and ethylene [38]. The efficiencies of ethylene formation is higher than methane at low current densities (1 mA/cm^2) and at high pH [39]. Kim et al. showed that methane and ethylene begins to form at -1.50 to -1.60 V vs SHE and methane is formed at a much lower rate from CO than from CO_2. The rate limiting step was suggested to be the electron transfer to adsorbed CO [40]. A similar study discovered that the electrode was poisoned by graphitic carbon which could be due to the decomposition of formate and a possible mechanism was suggested (Eq. 15) [18]. Cook et al. proposed that formaldehyde, formic acid and acetaldehyde are possible intermediates in the formation of hydrocarbons and reported the formation of carbon deposits on the electrodes in the reduction of formic acid [16].

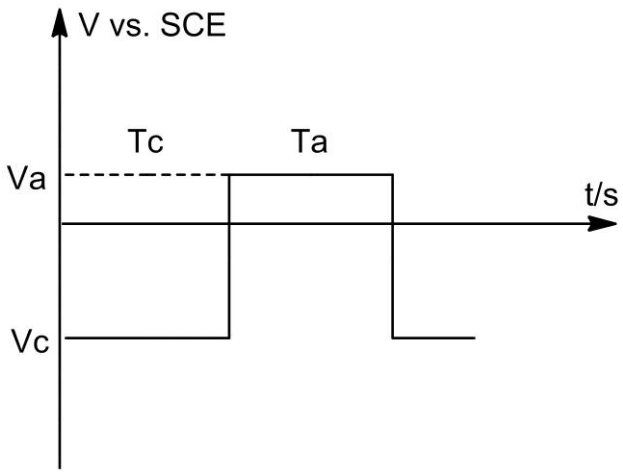

Fig. 4 Pulsed electroreduction technique where T_c and T_a represent the time cathodic and anodic biases (V_c, V_a) are applied, respectively.

Adsorption of amorphous carbon was also reported to occur within 1 hr of electrolysis which can be prevented by modulating the potential which causes the structure of the copper surface to change [41]. This method of potential modulation or pulsed potential was developed by Nogami et al. and was shown to perform much better than conventional electroreduction [42, 43]. Faradaic efficiencies for methane and ethylene were relatively constant throughout the process. Peak efficiency of 55% and 10% for methane and ethylene, respectively, was achieved at 10 °C with a high applied cathodic potential of -2.60 V vs SHE. This process is illustrated in Fig. 4. Applying this method to the CuAg (Cu/Ag = 28/72) alloy electrode seems to suggest that it is possible to control the product selectivity especially towards C_2 products such as ethylene, ethanol and acetaldehyde [44]. Total efficiency for the C_2 products was approximately 50% and was suggested that an oxide layer was formed and caused hydrogen atoms to desorb. In addition, the difference in adsorption on Cu and Ag may play a role in the improved C_2 efficiency.

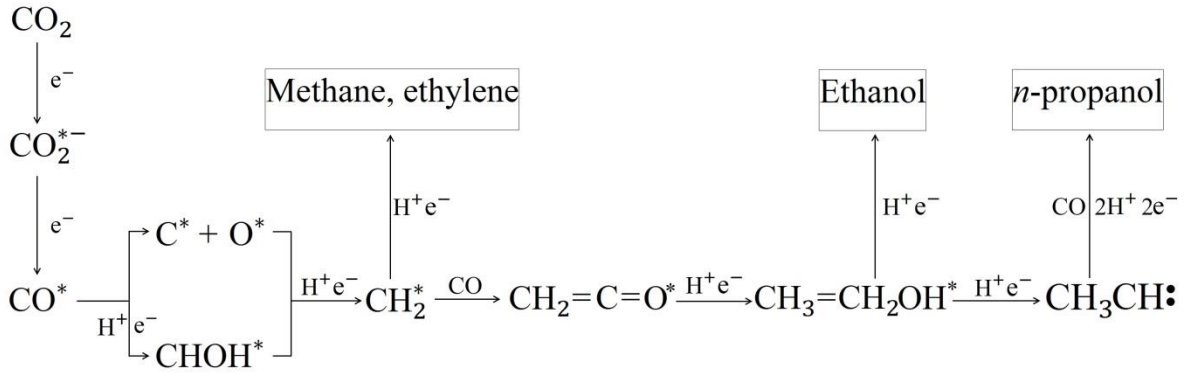

Fig. 5 Possible mechanism for the formation of methane, ethylene, ethanol and propanol with copper as [14].

An attempt to overcome the poisoning by carbon adsorption was by electroplating the copper electrodes with gold. However, electroplating of the electrodes resulted in the reduction in current efficiencies for hydrocarbons and alcohols but an increase for CO and H_2 with increasing in gold coverage [45]. Similar results were observed with copper-gold alloy electrodes [46]. The poisoning phenomena were later proved to be not caused by any of the adsorbed products but by the impurities such as Fe^{2+} and Zn^{2+} present in the electrolyte solutions [47].

$$CO_2 \rightarrow CO \rightarrow Cu\text{-}HCO \rightarrow Cu{=}CH_2 \rightarrow \text{hydrocarbons} \qquad (15)$$

It is evident from these early studies of aqueous electrochemical reduction of CO_2 with copper electrodes that methanol is not formed or detected in any of the studies. However, in the industry, one of the main catalysts for methanol production is copper supported on zinc oxide (Cu/ZnO) with additional promoters [48]. The reason behind this is still unclear at the time. To further understand the process, an in-depth study was performed by Hori et al. [14]. The study conducted at ambient temperature (19 °C), ethanol and propanol in addition to methane and ethylene were detected as products. It was proposed that CO_2 was reduced to CO and $HCOO^-$ at potentials more positive than -1.10 V vs SHE. The adsorbed CO inhibits

the evolution of H_2 and undergoes further reduction to hydrocarbons and alcohols when higher potentials are applied. The formation of ethylene and alcohols is also much more favourable when inorganic salts are used as electrolytes. Methane formation is much more favourable when more hydrogen atoms are available on the electrode surface. Finally, it was concluded that adsorbed CO binds weakly to the surface of the electrode. The overall proposed mechanism is illustrated in Fig. 5 which is similar to the Fischer-Tropsch process.

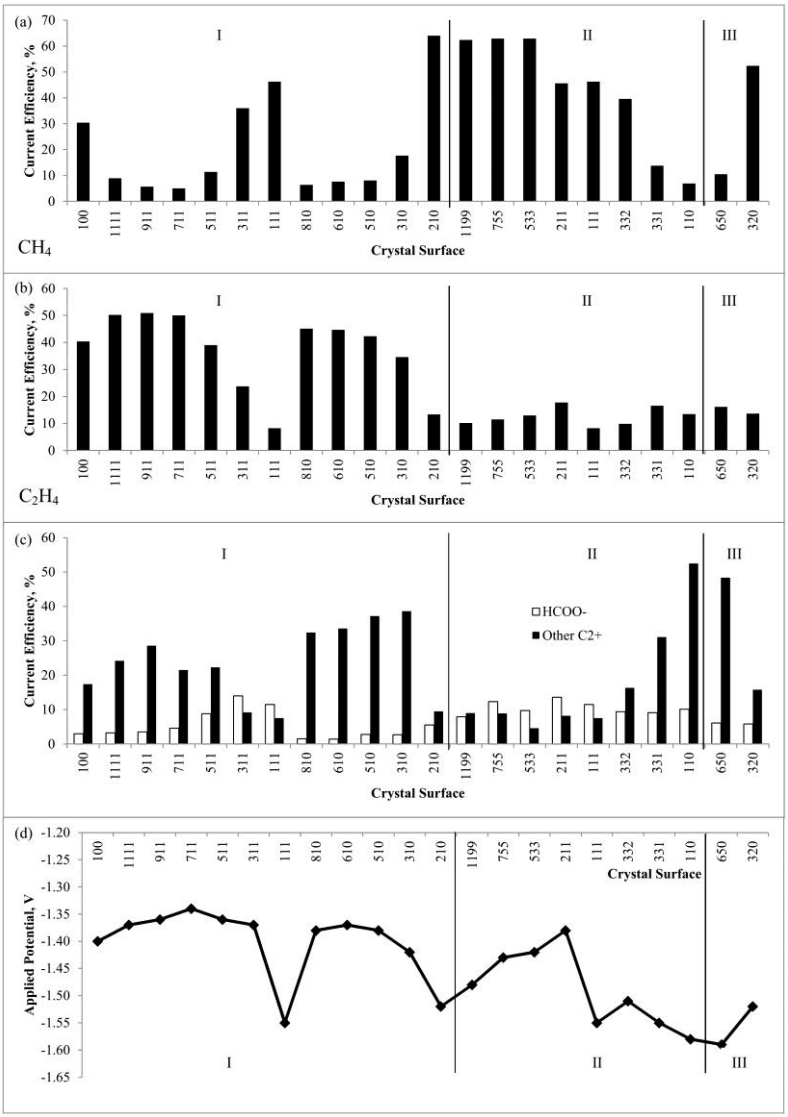

Fig. 6 Current efficiencies for formation of (a) methane, (b) ethylene, (c) formate and other C_{2+} products and (d) applied potential for various crystal series electrodes. Roman numerals (I), (II) and (III) indicate Cu(100), Cu(111) and Cu(110) dominant surfaces, respectively [49].

Hara et al. demonstrated that it was possible to control the selectivity of the reduction products by manipulating the pressure of CO_2, current density and stirring. The increase in CO_2 pressure, current density and absence of stirring improved the current efficiency for methane and ethylene formation while decreased the efficiency for formic acid and CO formation and vice versa [50]. Hori et al. was the first to report on the formation of acetic acid when using single crystal electrodes [51-53]. Acetic acid and other C_{2+} hydrocarbons were detected when the Cu(110) surface is the dominant surface. The Cu(111) dominant surface is much more selective in the formation of methane while the Cu(100) dominant surface is much more selective to ethylene. The summary of the current efficiencies of the products formed on various crystal series electrodes is illustrated in Fig. 6 [49]. Other than crystal facets alone, surface morphology of the electrodes play an important role in the selectivity as well. An electrode covered with copper nanoparticles has higher selectivity towards hydrocarbons as compared to an electropolished and a surface sputtered electrode which could be due to the higher number of uncoordinated sites present due the rough morphology [54].

Recent work by Reske et al. that focused on hydrocarbon (methane and ethylene) selectivity showed that Cu overlayers on Pt electrodes greater than 15 nm will exhibit characteristics similar to that of bulk Cu while monolayer Cu will have much less [55]. The decrease in Cu overlayer thickness results in the reduction in hydrocarbon selectivity. Little change towards hydrocarbon selectivity was observed for monolayer Cu when the applied potential was increased while there was a sharp increase in methane selectivity and moderate decrease in ethylene selectivity for both 5 nm and 15 nm overlayers. The combination of both surface strain (from lattice mismatch of Pt and Cu) and electronic effects is believed to play a role in the observed selectivity.

Recently, a new mechanism for formation of methane and ethylene in the electrochemical reduction of CO_2 was proposed by Schouten et al. [56] (see Eq. 16-18). The rate determining step for both methane and ethylene formation is the electron transfer to CO_2. For methane formation, it was proposed that the important intermediate is the CHO molecule instead of the COH as proposed by Hori et al. [14] which allows for the breaking of the C-O bond thus forming methane. The pathway for ethylene formation was suggested to occur from the dimer of two CO molecules. This dimerization would then proceed to form an enediol, enediolate or oxametallacycle and then the final product, ethylene. Two possible pathways toward ethylene formation were later proposed [57]. The formation of ethylene on the Cu(111) surface shares a common intermediate involved in the formation of methane while the formation proceeds through the dimerization pathway on the Cu(100) surface. More C_2 and C_3 species products (glyoxal, hydroxyacetone, glycoaldehyde, ethylene glycol and acetone) were also identified [15]. Possible mechanisms for the formation of C_2 and C_3 species were proposed but it is not clear how the C-C coupling occurs.

$$\text{Route 1: } CO_2 \rightarrow CO_2^{*-} \rightarrow HCOO^- \tag{16}$$

$$\text{Route 2: } CO_2 \rightarrow CO_2^{*-} \rightarrow CO^* \rightarrow HCO^* \rightarrow CH_2^* \rightarrow \text{methane} \tag{17}$$

$$\text{Route 3: } CO^* + CO^* \rightarrow \text{enediol/enediolate/oxametallacycle} \rightarrow \text{ethylene} \tag{18}$$

The selectivity of copper electrodes towards ethylene and current density was enhanced greatly and hydrogen evolution was greatly suppressed when halide ions were present in the electrolyte [58-60]. Higher concentrations of halide ions improve the current efficiency of ethylene formation and suppress hydrogen evolution further. A current efficiency for ethylene formation of up to 80% is achievable when copper(1) halides are confined within the copper mesh electrodes [58]. Ethylene is proposed to be formed through the coupling of adsorbed COOH [59]. Stronger bonding of the halide ions with the electrode

($Cl^- < Br^- < I^-$) may have contributed to the improved current efficiency of up to 13.2 mA/cm^2 by increasing the stability of adsorbed CO_2 thus allowing it to be protonated [60].

The use of thin copper oxide layer on the electrodes had also attracted some attention due to its ability to reduce CO_2 to methanol [61, 62]. Frese showed that the faradaic efficiency on various types of intentionally oxidised copper electrodes was high (up to 240%) at low current densities. p-Cu_2O was proposed to be responsible for the high selectivity towards methanol [61]. Cu_2O electrodeposited onto Cu foils performed better than air-oxidised and anodised Cu electrodes with two orders of magnitude greater in the production of methanol at about -1.60 V vs SHE of applied potential. The Cu_2O was also found to be reduced to metallic Cu in the process [62]. Both of these studies suggests that Cu(1) may play a critical role in the production of methanol but the stability of the oxides may require further investigation.

Despite the potential of copper oxides, there are some studies that did not report any methanol formation when copper oxide was present [63, 64]. Terunuma et al. reported that H_2 was the major product with very low amounts of methane and ethylene. A more recent study showed that methane formation was suppressed while enhancing the selectivity towards C_2 hydrocarbons [64]. Li et al. suggested that the absence of methane formation was due to the use of high annealing temperature of 500 °C (compared to ~300 °C [61, 62]) to produce the oxide layer.

The viability of combining electrical energy from solar cells in the electrochemical reduction of CO_2 was investigated by Peng et al. together with the possibility of degrading azo-dyes [65]. Products that were detected are methanol, methane, formaldehyde, formic acid and hydrogen. Current efficiencies for this setup were very low for all products compared to the earlier study by Hori et al. [14] except hydrogen. The formation of methanol could be due to the high voltage supply of -4.00 V vs SHE supplied by the solar cell. Although

improvements in current efficiencies were observed for carbon based products when methanol was added to the electrolyte, it is still much lower than in the study by Hori et al. [14].

Density functional theory (DFT) studies were applied to further understand the mechanism in the formation of CO_2 reduction production. DFT study of methane formation not only suggested a new possible mechanism but also uncovers a possible reason why methanol is not detected or detected in very low concentrations in electrochemical reduction of CO_2. The most favourable pathway for methane formation is proposed by Peterson et al., as shown in Eq. 19 [66]. Further modelling studies showed that the intermediates are most stable on the Cu(211) followed by Cu(100) and Cu(111) without any change to the reaction pathway [67]. This result was somewhat consistent with the single crystal study by Hori et al. [53] where the Cu(211) surface required the lowest applied potential to achieve a current density of 5 mA/cm^2 compared to Cu(100) and Cu(111). The mechanism was pointed out by Schouten et al. that it was not consistent with their experimental results [56]. However, it still supported that CHO as one of the intermediates for methane formation. Methane formation was favoured thermodynamically by 0.27 eV which translates to a molar excess of 40000:1. Materials having a similar binding strength to stabilise the CO and CHO intermediate were proposed to be necessary to improve the efficiency of the process [66].

$$CO_2 \rightarrow COOH \rightarrow CO \rightarrow CHO \rightarrow CH_2O \rightarrow CH_3O \rightarrow CH_4 \quad (19)$$

The discrepancy between experimental and computational observations was due to the models used in the computation [68]. The results obtained from the hydrogen-shuttling model closely resembled experimental observations. However, COH was suggested to be the important intermediate (similar to Hori et al. [14]) instead of CHO (Eq. 20). This pathway only exists in the aqueous electrochemical process as there is a lack of an aqueous environment in syngas methanol synthesis.

$$CO_2 \rightarrow COOH \rightarrow CO \rightarrow COH \rightarrow C \rightarrow CH_x \quad (20)$$

Further studies of C-C coupling revealed that the dimerization of CO is kinetically unfavourable [69]. CO has to be protonated to form CHO for favourable kinetics of C-C coupling to occur. Montoya et al. suggested that there is equilibrium between three intermediates (CHO, OHCCHO and CH_2O). The shift of equilibrium can be caused by the applied potentials which proceed to form methane and ethylene.

A DFT study on the effects of CO_2 adsorption and surface oxygen vacancy on the $Cu_2O(111)$ surface was carried out recently [70]. It was calculated that the oxygen vacancy is an active site for CO_2 radical formation. However, the presence of the vacancy also reduced the ability of CO_2 to adsorb onto unsaturated Cu and O sites. In addition, the dissociative adsorption was found to be thermodynamically unfeasible on this surface.

The same model used by Peterson et al. [66] was used by Hirunsit to understand the mechanisms for methane formation on alloys of copper (Cu_3Au and Cu_3Ag) [71]. The mechanistic pathway is similar for both Cu(211) and $Cu_3Ag(211)$ with Cu_3Ag being slightly more efficient. The rate limiting step is the protonation of the adsorbed CHO for both Cu(211) and $Cu_3Ag(211)$; and the protonation of adsorbed CO for $Cu_3Au(211)$. Although the formation of adsorbed OH was much more suppressed on the alloys, adsorbed CO is much more likely to desorb from the alloys compared to pure Cu. Adsorbed CO, CHO, HOCO and OH are important intermediates for a more effective catalyst.

Although pure copper does not exhibit the selectivity toward the formation of methanol at standard conditions, some modification to the system was shown to be able to produce methanol. Watanabe et al. demonstrated that the copper alloys of Cu-Cd (Cu/Cd = 38/62) and Cu-Ni (Cu/Ni = 90/10) was able to produce methanol [72]. A current efficiency of 7% and 5% and applied potentials of -0.38 and -1.75 V vs SHE was achieved for the formation of methanol on Cu-Ni and Cu-Cd electrodes, respectively. The change of Cu-Ni

ratio to 60/40 resulted in an increase in the current efficiency for methanol to 10% at the same applied potentials [73]. The modification of Ru electrodes with Cu also resulted in the formation of methanol in aqueous electrolyte with current efficiencies reaching up to 40% after 8 hours of electrolysis with only -0.80 V vs SHE of applied potential [74]. Other than the modification of the electrodes, it is also possible to produce methanol with a pressured ethanol-water-LiCl mixture as the electrolyte and pure copper as the electrodes [75]. An efficiency of 40% and current density of 9.0 mA/cm^2 was achieved at -1.10 V vs SHE when the electrolysis is carried out at 68 atm. The exact mechanism for the formation of methanol is still unclear as methanol was not reported to form (except in high pressure electrolyte) when pure metallic electrodes were used.

3.2. Platinum

Extensive studies have been performed to study the adsorption of CO and CO_2 on platinum electrodes but with differing opinions. However, most of the studies agreed that some form of reduced CO_2 is present on the electrode as a product [76]. Studies on single crystal electrodes showed that flat platinum surfaces (i.e., Pt(100) and Pt(111)) have the lowest activity for CO_2 reduction to CO while high kink densities and stepped surfaces have the highest activity [77, 78]. Platinum electrodes modified with a composite of RuO_2/TiO_2 in the form of nanoparticles and nanotubes were able to produce methanol with high efficiencies of up to 60% at -0.8 V vs SHE [79]. Electrodes modified with the nanotube composite were much more selective (60.5%) in the production of methanol as compared to the nanoparticle counterpart (40.5%). This could be due to the better dispersion of RuO_2 on the TiO_2 nanotubes as compared to the nanoparticles thus providing more surface area for the electro-reduction to occur.

3.3. Palladium

A series of studies was carried out by Ohkawa et al. using hydrogenated palladium electrodes with applied potentials of -1.60 to -1.80 V vs SHE [80-83]. Hydrogenation and addition of copper to the palladium electrode increased the current efficiency for the production of CO and formic acid as compared to the unmodified electrodes [80, 81]. The increased in efficiency is due to the participation of adsorbed hydrogen. Surface morphology from the modification with copper had no effect on the efficiency when compared to unhydrogenated electrodes. Methanol was reported to have formed with very low Faradaic efficiency (1%). Methane and ethylene were also reported with efficiencies of 35% and 5%, respectively. The remaining products of CO and formic acid were formed with efficiencies of about 20% and 60%, respectively. The copper deposition may have suppressed the formation of H_2 which allows the hydrogenation of the adsorbed intermediates thus allowing the formation of reduction products [82].

Kolbe et al. showed that the reduction of CO_2 to CO or formic acid on palladium electrodes begins at about -1 V vs SHE accompanied by hydrogen evolution. At -1.40 V volatile CO is formed thus freeing the surface for further reduction of CO_2. At 0.50 V oxidation of adsorbates (CO or formic acid) occurs [84]. The effect of different crystal structures on the rate of CO_2 reduction to CO was studied by Hori et al. and found that the Pd(111) surface has the highest activity which is contrary to other Pt group metals (Pt, Rh, Ir) at -0.50 V vs SHE [85]. Moreover, the Pd electrodes were prone to poisoning the adsorbates [86].

3.4. Others

Oxide derived gold nanoparticles were shown to be able to reduce CO_2 much more efficiently than polycrystalline gold nanoparticles [87]. Oxide derived gold nanoparticles

begin to reduce CO_2 to CO at -0.25 V vs SHE with a current efficiency of 65% compared to the polycrystalline alternative which only begin at above -0.35 V vs SHE. At higher applied potentials of up to -0.50 V vs SHE, the efficiency increases to more than 96% for oxide derived gold and only about 80% for polycrystalline gold. Current density is an order of magnitude higher for oxide derived gold (2-4 mA/cm^2 compared to 0.3-0.5 mA/cm^2). In terms of stability, oxide derived gold nanoparticles are much more stable and is able to maintain activity although sintering occurred within 15 minutes of reduction. The electron transfer to adsorbed CO_2 was proposed to be the rate determining step on polycrystalline gold while hydrogen transfer by HCO_3^- to adsorbed CO_2 radical which indicates that adsorbed CO_2 radical is much more stable on oxide derived gold nanoparticles.

Lead (Pb) granules in a fixed bed reactor were used in conjunction with high pressures (up to 500 kPa) and temperatures (up to 80 °C) to electrochemically reduce CO_2 to formic acid [88]. Peak current efficiency using this setup was 94% at -1.80 V vs SHE. This result is similar to what has been reported by Hori et al. where Pb electrodes have high selectivity towards formate at ambient conditions [11]. Although the electrochemical reduction using Pb-granules in a fixed bed reactor does exhibit higher current efficiencies at higher temperatures and pressures compared to ambient conditions, such efficiencies were achievable under ambient conditions using Pb electrodes alone [11].

Electrodeposited tin (Sn) on carbon paper was used to create a gas diffusion electrode [89]. The formation of formic acid was only reported when operated at -1.60 V vs SHE and slightly elevated temperatures of 40 °C. Current efficiency was very low at only 18% compared to the regular Sn electrode used by Hori et al. which reported an efficiency of 88% at only -1.48 V [11].

Molybdenum (Mo) exhibits the unique ability to electrochemically reduce CO_2 directly to methanol [90]. When pre-treated with HCl together with voltage cycling between -1.20 and

+0.20 V, the electroreduction at -0.80 V vs SHE is able to achieve an efficiency of 370%. The disadvantage of Mo electrodes is that it suffers from corrosion during open circuit conditions.

Recently, a DFT study was performed on metal-functionalised porphyrin-like graphene [91]. Various types of metals such as late transition metals (Cu, Ag, Au, Ni, Pd, Pt, Co, Rh, Ir, Fe, Ru, Os), B, Al, Ga and Mg had been used as the active site. The best catalyst for the system was calculated to be Rh and Fe for production of methanol and methane, respectively, due to the low voltage requirements (-0.19 V and -0.93 V respectively). Despite being predicted to be able to reduce CO_2 at such low voltages, the system also suffers from a competing reaction where H* competes for the active site. It was suggested that CO to be used instead of CO_2 for the reduction due to the competing reaction.

4. Molecular Electrocatalysts

Various metal complexes such as copper [92-94], palladium [95-99], nickel [100-108] and cobalt [21, 109-116] have been reported to be able to catalyse the electrochemical reduction of CO_2. Benson et al. suggested that specific catalysts should be utilised in specific steps of the CO_2 electrochemical reduction process as metal complexes can provide high selectivity toward specific products such as methanol [20].

4.1. Copper Complexes

Copper complexes have been shown to be able to fixate CO_2 directly from air when the pH is above 7 [92, 94]. CO_2 fixated to the complexes will form carbamates when there is only one copper centre present while two copper centres will cause the formation of carbonates instead [94]. The reduction of CO_2 at the complex was shown to occur in between -1.00 to -1.25 V vs SHE [92]. A dinuclear copper complex synthesised by Angamuthu et al.

spontaneously captured and reduced CO_2 with applied potentials of only -0.03 V vs SHE. Two CO_2 molecules formed bridges between the copper complexes forming oxalate which is then extracted using lithium salt [93].

4.2. Palladium Complexes

Electrochemical reduction under anhydrous conditions begins at about -1.30 V when monodentate palladium complexes are used. Presence of water in the electrolyte produced hydrogen and formic acid but no CO was detected in both conditions [95]. Presence of pyridine and pyrazole ligands in the complexes could function as electron acceptors at suitable potentials. However, the increase in donor strength of the ligands enhanced the amount of CO and decreases the formic acid production [96].

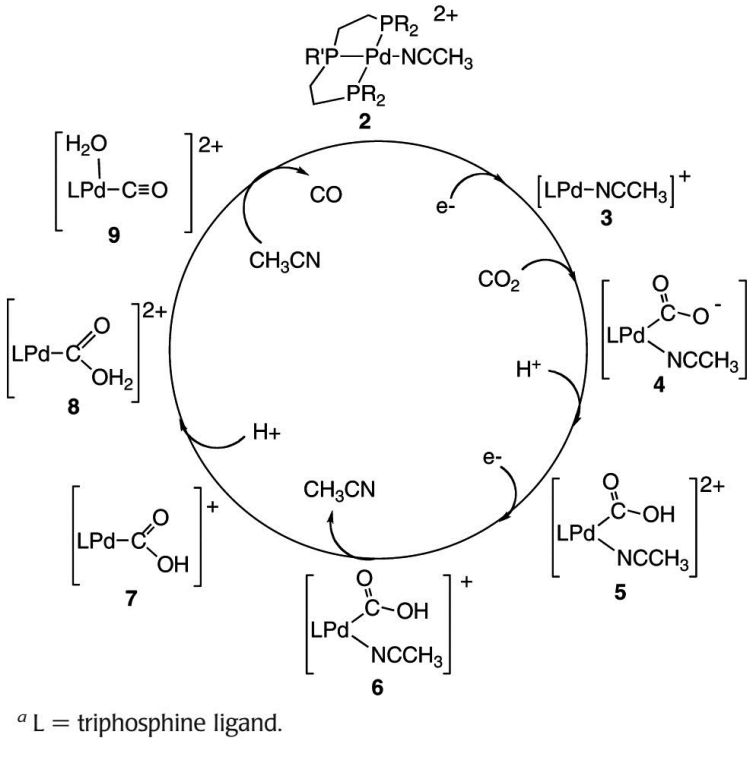

[a] L = triphosphine ligand.

Fig. 7 Proposed mechanism for electrochemical reduction of CO_2 using Pd complexes synthesised by DuBois et al. (Reproduced from ref. [99] by permission from the American Chemical Society).

DuBois et al. synthesised mono- and bipalladium phosphine complexes with palladium as reaction centres. The complex consists of a weakly binding solvent portion (i.e., acetonitrile) that will dissociate during catalysis revealing a vacant site for binding of water and assisting in the cleavage of C-O bond [97-99]. The reaction scheme for their catalyst is as shown in Fig. 7. The rate determining step is dependent on the concentration of acid present in the electrolyte. At high concentrations, the binding of CO_2 to the palladium site is the rate determining step (step 3→4) as H_2 production is much more favourable. On the other hand, the cleavage of the C-O bond (step 8→9) is rate determining and will require much higher potentials.

4.3. Nickel Complexes

Nickel cyclams have been shown to be highly selective in the reduction of CO_2 to CO under electrochemical conditions in water [100, 101]. Reduction of CO_2 was observed to begin at appreciably low potentials of -1.00 V with high turnover frequencies of approximately 1000 mol of CO per mol of nickel complex. The complex was very stable and does not degrade even after 10000 electrocatalytic cycles [100]. The efficiency of CO_2 reduction further improved with the use of dimetallic cyclams. The product was mainly CO when the reduction was carried out in water while high selectivity for formate was observed in a low water dimethylformamide (DMF) [101]. The use of mercury electrodes showed that the complexes are adsorbed onto the electrodes and remained to be the active catalyst in the reduction process [102-104]. However, the complexes will desorb when applied voltages are lower than -1.70 V vs SHE when CO or CO_2 is present. The reason is due to inability of the nickel-cyclam-CO complexes to adsorb onto the electrode [102, 104].

CO_2 was selectively reduced to oxalate with the use of other macrocyclic nickel complexes [106]. CO and carbonates were major products with low amounts of formate when

dinickel macrocyclic complexes was used to reduce CO_2 at about -1.00 V vs SHE [107]. Contrary to palladium complexes, dinickel macrocyclic complexes are less effective in reducing CO_2 due to steric effect of larger ligands. The activity was only half of that of mononuclear nickel macrocyclic complexes [105]. Nickel complexes of carbine-pyridine were also used to electrochemically reduce CO_2 in water with reduction occurring at applied potentials of -0.86 to -1.54 V. Although these complexes have high selectivity toward reducing CO_2 to CO, the production of CO is only moderate and deactivated when used continuously at high applied potentials [108]. Both formic acid and formaldehyde was detected when Ni-tetra-phthalocyanine (Ni-TaPc) was used [117]. Electroreduction was carried out at -1.0 V vs SHE and only the metal centre was reduced in the process.

4.4. Cobalt Complexes

Reduction potentials of CO_2 vary from -0.90 to -1.50 V vs SHE depending on the type of ligands of terdentate cobalt complexes in DMF [109-111]. The degree of conjugation of the ligands influences the stability and reactivity of the metal complexes. A reduction potential of -0.87 V is observed with formaldehyde as the sole product in aqueous media [114]. Immobilisation of the cobalt complexes to a dual-film electrode yielded methanol, ethanol, acetone and lactic acid at low potentials of -0.60 V vs SHE under ambient aqueous conditions [112, 113]. The products were not only detected in the solutions but also within the electrodes itself suggesting that the reduction process takes place at the electrode/solution interface and the active centres within the electrode. It was proposed that the reduction process proceeds via a stepwise hydrogenation by adsorbed hydrogen and coupling of the intermediates [113].

Macrocyclic cobalt complexes (phthalocyanine, CoPc) were also studied in aqueous solutions. CO was produced as main products at low potentials of -1.00 V vs SHE when

attached to glassy carbon electrodes. However, the efficiency was low at only 20% [116]. Similar results were observed using CoPc complexes trapped in a polyvinylpyridine membrane attached to a graphite electrode. A CO/H_2 ratio of 6.0 was achieved at applied potentials of -1.20 V vs SHE. The selectivity is highly dependent on the concentration of the CoPc complex within the membrane [115]. Gas diffusion electrodes modified with CoPc complexes were prepared to produce urea. The production of CO was at 99% efficiency but no urea was formed with an applied potential of -1.50 V vs SHE in the presence nitrate ions and CO_2. It was concluded that the CoPc complexes were not able to reduce nitrate ions to nitride ions (necessary intermediate to produce urea) and then to ammonia [21]. Reduction of applied potentials to -0.18 V vs SHE produced only formic acid with current efficiencies of 72% was observed when the CoPc complex was supported on polypyrrole (CoPc/PPy). This could be due to the improved hydrogen adsorption on the CoPc/PPy electrodes [118]. Co-tetra-aminophthalocyanine (Co-TaPc) was able to selectively reduce CO_2 to formic acid in aqueous solution with only -1.0 V vs SHE of applied potential [117]. In this process, both the active Co centre and the ligand underwent reduction compared to the Ni-TaPc complex where only the metal underwent reduction.

DFT studies have been employed to better understand the mechanisms in the electrochemical reduction of CO_2 with macrocyclic cobalt complexes. Leung et al. used hybrid functional and cobalt porphyrin (CoP) as their model molecule [119, 120]. Calculations showed that the ground state for $[CoP]^+$ (where P represents the porphyrin group) is not planar and have a Co-N bond distance of 1.947 Å. The key intermediate of the reduction process is $[CoP\text{-}COOH]^-$ [120] and an increased interaction of CO_2 with water helps to stabilise the intermediate. The calculated activation energy for C-OH bond cleavage is 5.2 kcal/mol and the rate determining step was suggested to be the electron transfer from the electrodes to the complexes [119].

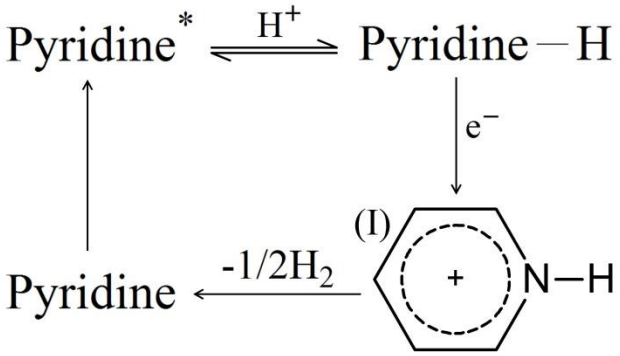

Fig. 8 Possible mechanism for the regeneration of the pyridinium catalyst [121].

4.5. Pyridinium

Pyridinium was found to be able to efficiently reduce CO_2 with low applied potentials. Methanol was detected when used in conjunction with hydrogenated palladium electrodes with efficiencies of up to 30% [121]. Reduction potentials were approximately -0.76 V vs SHE for methanol and -1.00 V for formaldehyde. A possible mechanism for the regeneration of the pyridinium catalyst is illustrated in Fig. 8. The reduction of CO_2 to methanol requires the transfer of six electrons with pyridinium functioning as a hydrogen shuttle [122]. Further studies using platinum electrodes revealed an activation barrier of 69±10 kJ/mol for CO_2 reduction. The electrons in the pyridinium ion were suggested to be concentrated at the nitrogen atom and the electron density reduced after reduction. The intermediate, pyridinium-CO_2, a carbamate-like species was proposed to be the rate determining step for the process [123].

Using DFT and continuum solvation model, Keith et al. showed that the pyridinyl radical (Fig. 8(I)) is not the active intermediate responsible for CO_2 reduction and should not form during the process as it would require an applied potential of -1.53 V [124]. Further calculations revealed that a more probable intermediate is the dihydropyridine (DHP) as the calculated reduction potential of -0.72 V is much closer to experimental values of -0.58 V vs SHE [125]. DFT study for the formation of formic acid revealed that the pyridinium cation

was first reduced by adsorbing the hydrogen to the electrode surface which is susceptible to electrophilic attack by CO_2 (Eq. 21). The reaction then proceeds with a two electron proton coupled hydride transfer thus forming formic acid (Eq. 22) [126].

$$\mathrm{PyrH^+ + Pt + e^- \rightarrow Pyr + Pt\text{-}H} \quad (21)$$

$$\mathrm{CO_2 + Pt\text{-}H + PyrH^+ \rightarrow Pyr + Pt + HCO_2H} \quad (22)$$

5. Photoelectrochemical and Bioelectrochemical Reduction

Photoelectrochemical reduction of CO_2 utilises the combination of a semiconductor and a molecular catalyst. Reported types of semiconductor used were p-Si [127-131], p-GaAs [132-134], p-InP [135, 136] and p-GaP [133, 137]. Metallic molecular catalysts used were mostly nickel [130, 131], cobalt [130, 131], ruthenium [136] and rhenium [128, 129] while non-metallic molecular catalysts were the enzyme formate dehydrogenase [135] and pyridine [137]. Most of the reduction is carried out under acidic conditions (pH 4.5-5.2) except for the enzyme based electroreduction where the pH was close to neutral (pH 6.8). Products formed from this method of electrochemical reduction are generally CO, formate, formaldehyde and methanol. Current efficiencies for reduction products are generally very good (50-100%) with applied voltages ranging from -0.02 to 1.75 V vs SHE.

Some notable ones are p-Si with Re complex, p-GaP(111) with pyridine and nickel cyclam and p-InP with formate dehydrogenase. The combination of p-Si photocathode with Re based complex achieved the formation of CO with a current efficiency of 100% in an anhydrous electrolyte. However, the applied voltage is quite high at about -1.75 V vs SHE [128, 129]. The use of p-GaP(111) with pyridine has high selectivity toward methanol in aqueous electrolyte with low applied voltage (-0.3 to -0.7 V vs SHE). Despite the high selectivity (up to 90%) toward methanol, the current density is very low of about 1.1 mA/cm^2 [137]. On the other hand, the combination of p-GaP(111) with dichloronickel cyclam

([Ni(cyclam)Cl_2]) in aqueous electrolyte produced CO at 85% efficiency with very low applied voltage of -0.02 V vs SHE [133]. Only formate was formed at very high efficiencies of 80-93% at very low applied voltage of -0.05 V vs SHE when the enzyme, formate dehydrogenase, was used as the active molecular catalyst in aqueous electrolyte. However, the current density was very low of only 0.6 mA/cm^2.

In an attempt to overcome the input requirement in the electrochemical reduction of CO_2, Zhao et al. combined a microbial fuel cell (MFC) with a microbial electrolysis cell (MEC) utilising a graphite electrode modified with Co-TaPc with carbon nanotubes [138]. The main product for this setup was formic acid at a voltage of -0.50 V with a peak current efficiency of 77%. The system showed no degradation even after 10 four hour cycles of reduction was performed.

Recently, a current density of up to 3 A/cm^2 was achieved using stainless steel electrodes together with *geobacter sulfurreducens* [139]. Only -0.6 V vs SHE was applied and glycerol was the only product. The possible mechanism of the process is still unknown but was proposed to be the consumption of succinate due to the reduced CO_2 (Eq. 23).

$$1/2\ C_4H_6O_4 + HCO_3^- + 8H^+ + 7e^- \rightarrow C_3H_8O_3 + 2H_2O \quad (23)$$

Table 1. The electrochemical reduction products of CO_2 over various catalysts.

	Catalysts	Products
Solid Oxide Fuel Cells	Platinum	CO
	Nickel	CO, methane
	Palladium	CO
	Copper	CO
Metallic Electrodes in Aqueous Solution	Copper	Hydrocarbons, CO, formate, alcohols
	Platinum	CO, methanol
	Palladium	CO, formic acid
	Others (Pb, Oxide-derived Au)	CO, formate
Molecular Electrocatalysts	Copper complexes	Oxalate
	Palladium complexes	CO, formic acid
	Nickel complexes	CO, oxalate, formic acid, formaldehyde
	Cobalt complexes	CO, formic acid, alcohols
	Pyridinium	Methanol, formaldehyde, formic acid
Photoelectrochemical and Bioelectrochemical Reduction	Semiconductor with molecular catalysts	CO, methanol, formate
	Microbial fuel cell with microbial electrolysis cell	Formic acid
	Stainless steel electrode with bacteria	Glycerol

6. Future Outlook and Summary

The potential uses of CO_2 to produce important chemicals and feedstocks are vast. The most important aspect in the utilisation of CO_2 is the reduced dependence on fossil fuels and reduction of atmospheric CO_2. Despite the impact that it can have on our environment, it has yet to be widely employed. All solutions in this discussion require some sort of energy input for the system to work as CO_2 is an extremely stable molecule. The products obtainable from electrochemical reduction of CO_2 using fuel cells, metal electrodes in aqueous electrolyte and molecular catalysts summarise in Table 1. For solid oxides, high temperatures are required in order for the solid electrolyte to be permeable towards oxygen ions. Due to the high temperatures, the major product tends to be CO. Although it is possible to produce methane, it requires the fuel cell to be run under electrolyser mode that requires an additional applied potential. The stability of the electrodes is also a main concern as it may undergo deactivation at such temperatures. The main benefit of using SOFCs is the ability in generating high current densities with reasonable voltages thus power.

On the other hand, low temperature CO_2 reduction requires an applied voltage and generally has low current densities. The most straight forward method is through electrolysis and the products are dependent on the type of the electrodes used. Copper and its oxide Cu_2O has gained a lot of interest as it is able to produce a wide range of hydrocarbons and oxygenates as products with high efficiency. Nanostructured copper such as nanoparticles and nanoarrays may provide suitable crystal facets or surfaces tuned to produce specific product for efficient electroreduction of CO_2. The actual mechanism is still a work in progress though recent studies have begun to unveil the possible process that is occurring. Despite having such unique properties to electrochemically reduce CO_2, it is still prone to poisoning from trace elements present in the electrolyte. Surface modification, alloying and

voltage modulation could potentially improve the performance of Cu electrodes by delaying the onset of deactivation but a more permanent solution is needed.

Various complexes have been proposed having extremely high activity toward CO_2 capture and reduction, in particular cobalt and nickel complexes. Required applied potentials are much lower than that of metal electrodes while reported products are generally CO and formic acid. Some complexes exhibit good stability and activity while there are some that degrade through extensive use. The mechanism involved is still a work in progress as there are many types of complexes synthesised but there is a general understanding of possible mechanism that is taking place. Pyridinium shows good potential in the electrochemical reduction process with reduction occurring at potentials of <1.00 V vs SHE. However, most experimental and modelling studies are based on platinum and palladium electrodes. For possibility of commercialisation a much cheaper electrode with comparable performance would be necessary.

The stability of the possible intermediates formed during the reduction process is important as it will influence the energy or voltage requirement of the system. Mechanistic studies will help to uncover the possible intermediates thus allowing for better electrocatalyst design. DFT studies have uncovered possible mechanisms that closely matched some experimental observations but there still remain some disagreements on what could actually be going on. Possible methods in stabilising intermediates in the case for methane formation in aqueous electrolyte are alloying of electrodes, stabilisation using ligand, tethering and additional promoters on the electrode [140]. Increased stability of key intermediates should require much lower applied voltages and more favourable protonation of the intermediate.

Acknowledgements

We acknowledge financial support from the Ministry of Education's academic research fund AcRF tier 1 (RG8/12 and RG73/10), Singapore. R. J. Lim is grateful to NTU for a scholarship. This publication is made possible by the Singapore National Research Foundation under its Campus for Research Excellence and Technological Enterprise (CREATE) programme.

References

[1] C. Keeling, S. Piper, R. Bacastow, M. Wahlen, T. Whorf, M. Heimann, H. Meijer, Atmospheric CO2 and 13CO2 Exchange with the Terrestrial Biosphere and Oceans from 1978 to 2000: Observations and Carbon Cycle Implications, in: I.T. Baldwin, M.M. Caldwell, G. Heldmaier, R. Jackson, O.L. Lange, H.A. Mooney, E.D. Schulze, U. Sommer, J. Ehleringer, M. Denise Dearing, T. Cerling, (Eds.), A History of Atmospheric CO2 and Its Effects on Plants, Animals, and Ecosystems, Springer New York, 2005, pp. 83-113.

[2] J. Ewald, Carbon Dioxide at NOAA's Mauna Loa Observatory reaches new milestone: Tops 400 ppm, National Oceanic and Atmospheric Administration, 2013.

[3] S. Solomon, J.S. Daniel, T.J. Sanford, D.M. Murphy, G.-K. Plattner, R. Knutti, P. Friedlingstein, Proceedings of the National Academy of Sciences 107 (2010) 18354-18359.

[4] S. Solomon, G.K. Plattner, R. Knutti, P. Friedlingstein, Proceedings of the National Academy of Sciences of the United States of America 106 (2009) 1704-1709.

[5] D. Archer, V. Brovkin, Clim. Change 90 (2008) 283-297.

[6] M. Aresta, A. Dibenedetto, Catal. Today 98 (2004) 455-462.

[7] Key World Energy Statistics 2012, 2012, pp. 1-80.

[8] M. Specht, F. Staiss, A. Bandi, T. Weimer, Int. J. Hydrogen Energy 23 (1998) 387-396.

[9] T. Weimer, K. Schaber, M. Specht, A. Bandi, Energy Convers. Manage. 37 (1996) 1351-1356.

[10] M.E. Dry, Catal. Today 71 (2002) 227-241.

[11] Y. Hori, H. Wakebe, T. Tsukamoto, O. Koga, Electrochim. Acta 39 (1994) 1833-1839.

[12] T.-J. Huang, C.-L. Chou, Electrochem. Commun. 11 (2009) 1464-1467.

[13] Z. Zhan, L. Zhao, J. Power Sources 195 (2010) 7250-7254.

[14] Y. Hori, A. Murata, R. Takahashi, Journal of the Chemical Society, Faraday Transactions 1 85 (1989) 2309.

[15] K.P. Kuhl, E.R. Cave, D.N. Abram, T.F. Jaramillo, Energy & Environmental Science 5 (2012) 7050-7059.

[16] R.L. Cook, R.C. MacDuff, A.F. Sammells, J. Electrochem. Soc. 136 (1989) 1982-1984.

[17] M. Jitaru, D.A. Lowy, M. Toma, B.C. Toma, L. Oniciu, J. Appl. Electrochem. 27 (1997) 875-889.

[18] D.W. DeWulf, T. Jin, A.J. Bard, J. Electrochem. Soc. 136 (1989) 1686-1691.

[19] J.A. Dean, Lange's Handbook of Chemistry (15th Edition), McGraw-Hill, 1999.

[20] E.E. Benson, C.P. Kubiak, A.J. Sathrum, J.M. Smieja, Chem. Soc. Rev. 38 (2009) 89-99.

[21] M. Shibata, N. Furuya, Electrochim. Acta 48 (2003) 3953-3958.

[22] A. Choudhury, H. Chandra, A. Arora, Renewable and Sustainable Energy Reviews 20 (2013) 430-442.

[23] M. Lo Faro, A. Stassi, V. Antonucci, V. Modafferi, P. Frontera, P. Antonucci, A.S. Aricò, Int. J. Hydrogen Energy 36 (2011) 9977-9986.

[24] A.T. Ashcroft, A.K. Cheetham, M.L.H. Green, P.D.F. Vernon, Nature 352 (1991) 225-226.

[25] S. Furukawa, M. Okada, Y. Suzuki, Energy & Fuels 13 (1999) 1074-1081.

[26] F. Bidrawn, G. Kim, G. Corre, J.T.S. Irvine, J.M. Vohs, R.J. Gorte, Electrochem. Solid-State Lett. 11 (2008) B167-B170.

[27] T. Kim, S. Moon, S.-I. Hong, Applied Catalysis A: General 224 (2002) 111-120.

[28] D.J. Moon, J.M. Park, J.S. Kang, K.S. Yoo, S.I. Hong, Journal of Industrial and Engineering Chemistry 12 (2006) 149-155.
[29] K.R. Sridhar, B.T. Vaniman, Solid State Ionics 93 (1997) 321-328.
[30] S. Sridhar, V. Stancovski, U.B. Pal, Solid State Ionics 100 (1997) 17-22.
[31] G. Tao, K.R. Sridhar, C.L. Chan, Solid State Ionics 175 (2004) 615-619.
[32] G. Tao, K.R. Sridhar, C.L. Chan, Solid State Ionics 175 (2004) 621-624.
[33] Y. Shi, Y. Luo, N. Cai, J. Qian, S. Wang, W. Li, H. Wang, Electrochim. Acta 88 (2013) 644-653.
[34] M.J. Hei, H.B. Chen, J. Yi, Y.J. Lin, Y.Z. Lin, G. Wei, D.W. Liao, Surf. Sci. 417 (1998) 82-96.
[35] C.Y. Cheng, G.H. Kelsall, L. Kleiminger, J. Appl. Electrochem. (2013) 1-14.
[36] K. Xie, Y. Zhang, G. Meng, J.T.S. Irvine, J. Mater. Chem. 21 (2011) 195-198.
[37] Y. Hori, K. Kikuchi, S. Suzuki, Chem. Lett. 14 (1985) 1695-1698.
[38] Y. Hori, K. Kikuchi, A. Murata, S. Suzuki, Chem. Lett. 15 (1986) 897-898.
[39] Y. Hori, A. Murata, R. Takahashi, S. Suzuki, J. Am. Chem. Soc. 109 (1987) 5022-5023.
[40] J.J. Kim, D.P. Summers, K.W. Frese Jr, Journal of Electroanalytical Chemistry and Interfacial Electrochemistry 245 (1988) 223-244.
[41] J. Lee, Y. Tak, Electrochim. Acta 46 (2001) 3015-3022.
[42] R. Shiratsuchi, Y. Aikoh, G. Nogami, J. Electrochem. Soc. 140 (1993) 3479-3482.
[43] G. Nogami, H. Itagaki, R. Shiratsuchi, J. Electrochem. Soc. 141 (1994) 1138-1142.
[44] S. Ishimaru, R. Shiratsuchi, G. Nogami, J. Electrochem. Soc. 147 (2000) 1864-1867.
[45] G. Kyriacou, A. Anagnostopoulos, J. Electroanal. Chem. 328 (1992) 233-243.
[46] J. Christophe, T. Doneux, C. Buess-Herman, Electrocatalysis 3 (2012) 139-146.
[47] Y. Hori, H. Konishi, T. Futamura, A. Murata, O. Koga, H. Sakurai, K. Oguma, Electrochim. Acta 50 (2005) 5354-5369.
[48] J.B. Hansen, P.E. Højlund Nielsen, Methanol Synthesis, Handbook of Heterogeneous Catalysis, Wiley-VCH Verlag GmbH & Co. KGaA, 2008.
[49] M. Gattrell, N. Gupta, A. Co, J. Electroanal. Chem. 594 (2006) 1-19.
[50] K. Hara, A. Tsuneto, A. Kudo, T. Sakata, J. Electrochem. Soc. 141 (1994) 2097-2103.
[51] Y. Hori, H. Wakebe, T. Tsukamoto, O. Koga, Surf. Sci. 335 (1995) 258-263.
[52] I. Takahashi, O. Koga, N. Hoshi, Y. Hori, J. Electroanal. Chem. 533 (2002) 135-143.
[53] Y. Hori, I. Takahashi, O. Koga, N. Hoshi, J. Mol. Catal. A: Chem. 199 (2003) 39-47.
[54] W. Tang, A.A. Peterson, A.S. Varela, Z.P. Jovanov, L. Bech, W.J. Durand, S. Dahl, J.K. Norskov, I. Chorkendorff, PCCP 14 (2012) 76-81.
[55] R. Reske, M. Duca, M. Oezaslan, K.J.P. Schouten, M.T.M. Koper, P. Strasser, The Journal of Physical Chemistry Letters 4 (2013) 2410-2413.
[56] K.J.P. Schouten, Y. Kwon, C.J.M. van der Ham, Z. Qin, M.T.M. Koper, Chemical Science 2 (2011) 1902-1909.
[57] K.J.P. Schouten, Z. Qin, E.P. Gallent, M.T.M. Koper, J. Am. Chem. Soc. 134 (2012) 9864-9867.
[58] H. Yano, T. Tanaka, M. Nakayama, K. Ogura, J. Electroanal. Chem. 565 (2004) 287-293.
[59] K. Ogura, R. Oohara, Y. Kudo, J. Electrochem. Soc. 152 (2005) D213-D219.
[60] K. Ogura, J.R. Ferrell Iii, A.V. Cugini, E.S. Smotkin, M.D. Salazar-Villalpando, Electrochim. Acta 56 (2010) 381-386.
[61] K.W. Frese, J. Electrochem. Soc. 138 (1991) 3338-3344.
[62] M. Le, M. Ren, Z. Zhang, P.T. Sprunger, R.L. Kurtz, J.C. Flake, J. Electrochem. Soc. 158 (2011) E45-E49.
[63] Y. Terunuma, A. Saitoh, Y. Momose, J. Electroanal. Chem. 434 (1997) 69-75.

[64] C.W. Li, M.W. Kanan, J. Am. Chem. Soc. 134 (2012) 7231-7234.
[65] Y.P. Peng, Y.T. Yeh, P.Y. Wang, C.P. Huang, Sep. Purif. Technol. (2013).
[66] A.A. Peterson, F. Abild-Pedersen, F. Studt, J. Rossmeisl, J.K. Norskov, Energy & Environmental Science 3 (2010) 1311-1315.
[67] W.J. Durand, A.A. Peterson, F. Studt, F. Abild-Pedersen, J.K. Nørskov, Surf. Sci. 605 (2011) 1354-1359.
[68] X. Nie, M.R. Esopi, M.J. Janik, A. Asthagiri, Angew. Chem. Int. Ed. 52 (2013) 2459-2462.
[69] J.H. Montoya, A.A. Peterson, J.K. Nørskov, ChemCatChem 5 (2013) 737-742.
[70] H. Wu, N. Zhang, H. Wang, S. Hong, Chem. Phys. Lett. 568–569 (2013) 84-89.
[71] P. Hirunsit, The Journal of Physical Chemistry C 117 (2013) 8262-8268.
[72] M. Watanabe, M. Shibata, A. Kato, M. Azuma, T. Sakata, J. Electrochem. Soc. 138 (1991) 3382-3389.
[73] M. Watanabe, M. Shibata, A. Katoh, T. Sakata, M. Azuma, Journal of Electroanalytical Chemistry and Interfacial Electrochemistry 305 (1991) 319-328.
[74] J.P. Popić, M.L. Avramov-Ivić, N.B. Vuković, J. Electroanal. Chem. 421 (1997) 105-110.
[75] J. Li, G. Prentice, J. Electrochem. Soc. 144 (1997) 4284-4288.
[76] J. Sobkowski, A. Czerwinski, J. Phys. Chem. 89 (1985) 365-369.
[77] N. Hoshi, S. Kawatani, M. Kudo, Y. Hori, J. Electroanal. Chem. 467 (1999) 67-73.
[78] N. Hoshi, Y. Hori, Electrochim. Acta 45 (2000) 4263-4270.
[79] J. Qu, X. Zhang, Y. Wang, C. Xie, Electrochim. Acta 50 (2005) 3576-3580.
[80] K. Ohkawa, K. Hashimoto, A. Fujishima, Y. Noguchi, S. Nakayama, J. Electroanal. Chem. 345 (1993) 445-456.
[81] K. Ohkawa, Y. Noguchi, S. Nakayama, K. Hashimoto, A. Fujishima, J. Electroanal. Chem. 348 (1993) 459-464.
[82] K. Ohkawa, Y. Noguchi, S. Nakayama, K. Hashimoto, A. Fujishima, J. Electroanal. Chem. 367 (1994) 165-173.
[83] K. Ohkawa, Y. Noguchi, S. Nakayama, K. Hashimoto, A. Fujishima, J. Electroanal. Chem. 369 (1994) 247-250.
[84] D. Kolbe, W. Vielstich, Electrochim. Acta 41 (1996) 2457-2460.
[85] N. Hoshi, M. Noma, T. Suzuki, Y. Hori, J. Electroanal. Chem. 421 (1997) 15-18.
[86] C. Iwakura, S. Takezawa, H. Inoue, J. Electroanal. Chem. 459 (1998) 167-169.
[87] Y. Chen, C.W. Li, M.W. Kanan, J. Am. Chem. Soc. 134 (2012) 19969-19972.
[88] F. Köleli, D. Balun, Applied Catalysis A: General 274 (2004) 237-242.
[89] R.L. Machunda, H. Ju, J. Lee, Current Applied Physics 11 (2011) 986-988.
[90] D.P. Summers, S. Leach, K.W. Frese Jr, Journal of Electroanalytical Chemistry and Interfacial Electrochemistry 205 (1986) 219-232.
[91] V. Tripkovic, M. Vanin, M. Karamad, M.E. Björketun, K.W. Jacobsen, K.S. Thygesen, J. Rossmeisl, The Journal of Physical Chemistry C 117 (2013) 9187-9195.
[92] B. Verdejo, S. Blasco, J. González, E. García-España, P. Gaviña, S. Tatay, A. Doménech, M.T. Doménech-Carbó, H.R. Jiménez, C. Soriano, Eur. J. Inorg. Chem. 2008 (2008) 84-97.
[93] R. Angamuthu, P. Byers, M. Lutz, A.L. Spek, E. Bouwman, Science 327 (2010) 313-315.
[94] E. García-España, P. Gaviña, J. Latorre, C. Soriano, B. Verdejo, J. Am. Chem. Soc. 126 (2004) 5082-5083.
[95] A.G.M.M. Hossain, T. Nagaoka, K. Ogura, Electrochim. Acta 41 (1996) 2773-2780.
[96] A.G.M.M. Hossain, T. Nagaoka, K. Ogura, Electrochim. Acta 42 (1997) 2577-2585.
[97] B.D. Steffey, C.J. Curtis, D.L. DuBois, Organometallics 14 (1995) 4937-4943.

[98] J.W. Raebiger, J.W. Turner, B.C. Noll, C.J. Curtis, A. Miedaner, B. Cox, D.L. DuBois, Organometallics 25 (2006) 3345-3351.
[99] M. Rakowski Dubois, D.L. Dubois, Acc. Chem. Res. 42 (2009) 1974-1982.
[100] M. Beley, J.P. Collin, R. Ruppert, J.P. Sauvage, J. Am. Chem. Soc. 108 (1986) 7461-7467.
[101] J.P. Collin, A. Jouaiti, J.P. Sauvage, Inorg. Chem. 27 (1988) 1986-1990.
[102] M. Fujihira, Y. Hirata, K. Suga, Journal of Electroanalytical Chemistry and Interfacial Electrochemistry 292 (1990) 199-215.
[103] G.B. Balazs, F.C. Anson, J. Electroanal. Chem. 322 (1992) 325-345.
[104] G.B. Balazs, F.C. Anson, J. Electroanal. Chem. 361 (1993) 149-157.
[105] C. de Alwis, J.A. Crayston, T. Cromie, T. Eisenblätter, R.W. Hay, Y.D. Lampeka, L.V. Tsymbal, Electrochim. Acta 45 (2000) 2061-2074.
[106] M. Rudolph, S. Dautz, E.-G. Jäger, J. Am. Chem. Soc. 122 (2000) 10821-10830.
[107] E. Simón-Manso, C.P. Kubiak, Organometallics 24 (2004) 96-102.
[108] V.S. Thoi, C.J. Chang, Chem. Commun. 47 (2011) 6578-6580.
[109] C. Arana, S. Yan, M. Keshavarz-K, K.T. Potts, H.D. Abruna, Inorg. Chem. 31 (1992) 3680-3682.
[110] C. Arana, M. Keshavarz, K.T. Potts, H.D. Abruña, Inorg. Chim. Acta 225 (1994) 285-295.
[111] G. Chiericato Jr, C.R. Arana, C. Casado, I. Cuadrado, H.D. Abruña, Inorg. Chim. Acta 300–302 (2000) 32-42.
[112] K. Ogura, K. Mine, J. Yano, H. Sugihara, J. Chem. Soc., Chem. Commun. 0 (1993) 20-21.
[113] K. Ogura, H. Sugihara, J. Yano, M. Higasa, J. Electrochem. Soc. 141 (1994) 419-424.
[114] J.A. Ramos Sende, C.R. Arana, L. Hernandez, K.T. Potts, M. Keshevarz-K, H.D. Abruna, Inorg. Chem. 34 (1995) 3339-3348.
[115] T. Abe, T. Yoshida, S. Tokita, F. Taguchi, H. Imaya, M. Kaneko, J. Electroanal. Chem. 412 (1996) 125-132.
[116] H. Aga, A. Aramata, Y. Hisaeda, J. Electroanal. Chem. 437 (1997) 111-118.
[117] M. Isaacs, F. Armijo, G. Ramírez, E. Trollund, S.R. Biaggio, J. Costamagna, M.J. Aguirre, J. Mol. Catal. A: Chem. 229 (2005) 249-257.
[118] A. Zhang, W. Zhang, J. Lu, G.G. Wallace, J. Chen, Electrochem. Solid-State Lett. 12 (2009) E17-E19.
[119] K. Leung, I.M.B. Nielsen, N. Sai, C. Medforth, J.A. Shelnutt, The Journal of Physical Chemistry A 114 (2010) 10174-10184.
[120] I.M.B. Nielsen, K. Leung, The Journal of Physical Chemistry A 114 (2010) 10166-10173.
[121] G. Seshadri, C. Lin, A.B. Bocarsly, J. Electroanal. Chem. 372 (1994) 145-150.
[122] E. Barton Cole, P.S. Lakkaraju, D.M. Rampulla, A.J. Morris, E. Abelev, A.B. Bocarsly, J. Am. Chem. Soc. 132 (2010) 11539-11551.
[123] A.J. Morris, R.T. McGibbon, A.B. Bocarsly, Chemsuschem 4 (2011) 191-196.
[124] J.A. Keith, E.A. Carter, J. Am. Chem. Soc. 134 (2012) 7580-7583.
[125] J.A. Keith, E.A. Carter, Chemical Science 4 (2013) 1490-1496.
[126] M.Z. Ertem, S.J. Konezny, C.M. Araujo, V.S. Batista, The Journal of Physical Chemistry Letters 4 (2013) 745-748.
[127] B. Aurian-Blajeni, I. Taniguchi, J.O.M. Bockris, Journal of Electroanalytical Chemistry and Interfacial Electrochemistry 149 (1983) 291-293.
[128] B. Kumar, J.M. Smieja, C.P. Kubiak, The Journal of Physical Chemistry C 114 (2010) 14220-14223.

[129] C.R. Cabrera, H.D. Abruña, Journal of Electroanalytical Chemistry and Interfacial Electrochemistry 209 (1986) 101-107.
[130] M.G. Bradley, T. Tysak, Journal of Electroanalytical Chemistry and Interfacial Electrochemistry 135 (1982) 153-157.
[131] M.G. Bradley, T. Tysak, D.J. Graves, N.A. Viachiopoulos, J. Chem. Soc., Chem. Commun. 0 (1983) 349-350.
[132] M. Beley, J.-P. Collin, J.-P. Sauvage, J.-P. Petit, P. Chartier, Journal of Electroanalytical Chemistry and Interfacial Electrochemistry 206 (1986) 333-339.
[133] J.-P. Petit, P. Chartier, M. Beley, J.-P. Deville, Journal of Electroanalytical Chemistry and Interfacial Electrochemistry 269 (1989) 267-281.
[134] M. Zafrir, M. Ulman, Y. Zuckerman, M. Halmann, Journal of Electroanalytical Chemistry and Interfacial Electrochemistry 159 (1983) 373-389.
[135] B.A. Parkinson, P.F. Weaver, Nature 309 (1984) 148-149.
[136] T. Arai, S. Sato, K. Uemura, T. Morikawa, T. Kajino, T. Motohiro, Chem. Commun. 46 (2010) 6944-6946.
[137] E.E. Barton, D.M. Rampulla, A.B. Bocarsly, J. Am. Chem. Soc. 130 (2008) 6342-6344.
[138] H. Zhao, Y. Zhang, B. Zhao, Y. Chang, Z. Li, Environ. Sci. Technol. 46 (2012) 5198-5204.
[139] L. Soussan, J. Riess, B. Erable, M.-L. Delia, A. Bergel, Electrochem. Commun. 28 (2013) 27-30.
[140] A.A. Peterson, J.K. Nørskov, The Journal of Physical Chemistry Letters 3 (2012) 251-258.